IL NUOVO CIMENTO Vol. 34 C, N. 1 Gennaio-Febbraio 2011
DOI 10.1393/ncc/i2011-10822-1

Colloquia: IFA 2010

The ion microbeam facility of Florence: A versatile instrument for the analysis and modification of materials

M. Massi

INFN, Sezione di Firenze - via Bruno Rossi 1, 50019 Sesto Fiorentino (FI), Italy

(ricevuto l' 1 Luglio; approvato il 22 Luglio 2010; pubblicato online l'1 Marzo 2011)

Summary. — A brief description of the relevant features of the external scanning ion microbeam facility installed at the 3 MV tandem accelerator in Florence is here reported. With our facility we can work in "external" set-up (the target is kept in atmosphere) with a beam spot size on sample better than 10 μm. The Ion Beam Analyses (IBA) detection set-up of our microbeam allows us to exploit simultaneously PIXE (Particle-Induced X-ray Emission), PIGE (Particle-Induced γ-ray Emission), BS (Backscattering Spectrometry) and IBIL (Ion-Beam–Induced Luminescence) techniques; in combination with a scanning system, it is thus possible to fully characterize samples, through the collection of 2D maps of structural and elemental information. Finally, an activity recently started at the microbeam of Florence with regards to the ion modification of diamond is reported.

PACS 89.20.-a – Interdisciplinary applications of physics.
PACS 07.78.+s – Electron, positron, and ion microscopes;electron diffractometers.
PACS 07.79.-v – Scanning probe microscopes and components.
PACS 81.70.-q – Methods of materials testing and analysis.

1. – Introduction

Techniques for characterization of materials exploiting ion beams of energy of few MeV per nucleon from electrostatic accelerators are well established. The Ion Beam Analysis (IBA) techniques [1-3] exploit the products of interaction of a beam of charged particles with a target; detecting the emitted radiations, it is possible to obtain structural and compositional information on the sample. A very important feature, common to all IBA techniques, is the possibility of non-invasive and non-destructive analyses, thanks to the high sensitivity (down to part-per-million concentrations) of the techniques allowing measurements at low fluences (typically of the order of 10^{16} particles/cm^2), that generally do not lead to alterations of the sample. In addition, ion beams of such energies can be extracted from the vacuum pipeline by means of a very thin membrane (exit window) and the sample can be analysed while maintained in atmosphere [4].

An external beam set-up has many advantages compared to the conventional one with the target in vacuum: ease of handling and moving the target, whichever its size, much smaller risk of damage, reduced charging and over-heating effects or no effects at all. IBA techniques are typically applied in material science, earth science, cultural heritage, biology, medicine and environmental studies.

The use of an ion microprobe (ion beams with dimensions of less than $100\,\mu$m), to extract compositional and structural information with high spatial resolution from a small region in the sample, was an obvious development of these techniques [5]. This has been of great importance to samples that have elemental microstructures such as biological tissues, geological materials, microelectronic devices, or to tiny samples, for example cultured individual cells, microcrystals and single aerosol particles.

Ion microprobes are typically obtained by the strong focusing action of ion lenses, typically multiplets of magnetic quadrupoles.

Further, a significant step beyond was the use of a scanning system to control the beam position on the sample surface; it allows spatial distribution maps of elements within the analysed area to be imaged.

At the Laboratorio di Tecniche Nucleari per i Beni Culturali (LABEC) in Florence, an external scanning microbeam facility based on a magnetic quadrupole doublet is installed on a line of the 3 MV Tandetron accelerator. The use of external set-up with a microbeam limits the minimum beam dimensions due to the scattering of the particles in the extraction window and along the external path before hitting the target. However, the use of extremely thin windows and of as short as possible external paths saturated with helium allows us to limit this effect. At this facility it is possible to use an external beam with dimensions within $10\,\mu$m.

Some examples of IBA applications carried out at the microbeam of Florence are here briefly described.

An independent field of application of MeV ion microbeams which is gaining increasing interest is the ion modification of the physico-chemical properties of materials, for instance the ion beam lithography by means of microbeam writing [6] in the field of semiconductor electronics, or the study of the effects of radiation damage in biological samples [7]. Recently at LABEC microbeam we have started a study of refractive index change in diamond induced by ion damage and here it is briefly described.

2. – External scanning microbeam facility in Florence

2˙1. *External microbeam forming system.* – As mentioned before, MeV ion microprobes are formed by means of a strong focusing lens made by arranging quadrupoles in multiplets. Figure 1 shows the basics of a microbeam system, in which a short–focal-length lens L forms a demagnified image of an illuminated object aperture O in the image plane I. An adjustable aperture D controls the intensity of the beam and/or the aberration introduced by the lens. In order to form a demagnified image, the object distance O-L must be greater than the image distance L-I; to minimize the image dimensions the ratio L-I/O-L must be as small as possible. At the LABEC microbeam (fig. 2a) we have L-I ~ 0.2 m and O-L ~ 6 m and we use as a lens an Oxford Microbeams Ltd. OM100 quadrupole doublet [8] (fig. 2b).

Quadrupoles can be also arranged in triplets, quadruplets, quintuplets or even more complex configurations (Oxford triplet, "Russian" quadruplet, separated quintuplet [9], double doublet with superconducting quadrupoles at the second stage [10] and double triplet [11, 12]). The best spatial resolutions reported for IBA measurements are in

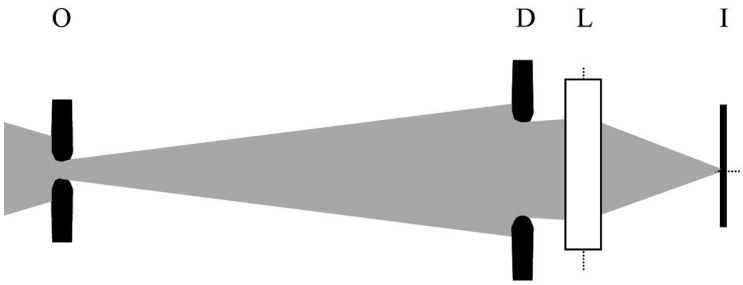

Fig. 1. – Scheme of a focusing system: L is a strong focusing lens which forms the image of the object O at the plane I. The diaphragm D controls the intensity of the beam arriving on the lens L and limits the aberrations introduced by L.

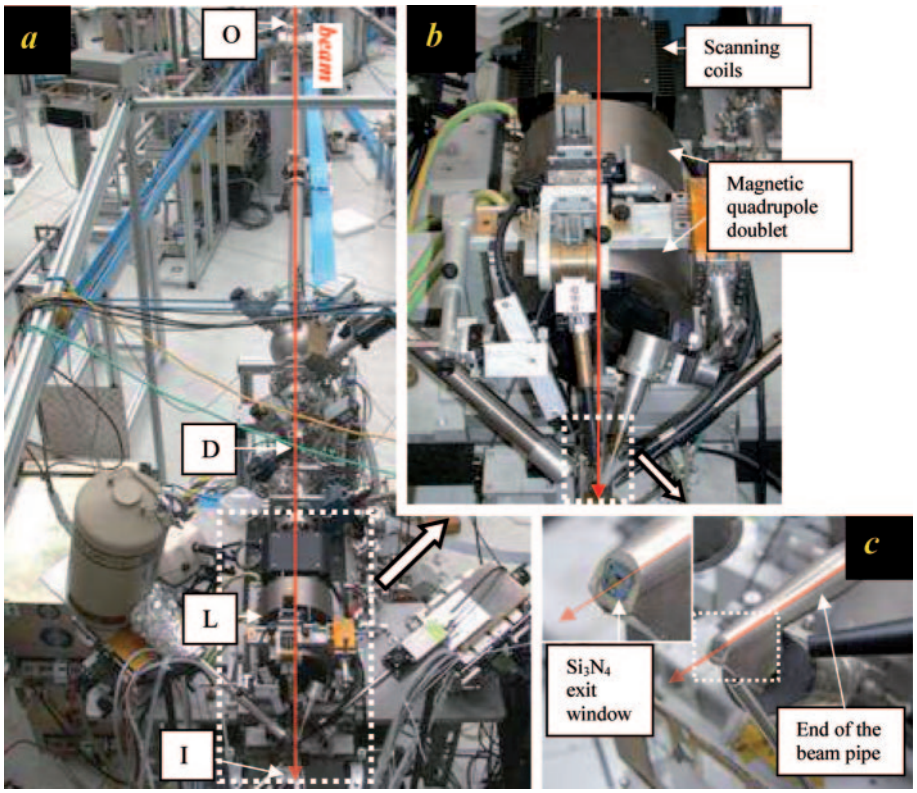

Fig. 2. – (a) General overview of the LABEC microbeam line, (b) strong focusing lens and scanning coils and (c) the end of the microbeam line with a blow-up on the beam extraction Si_3N_4 window (the dashed line rectangle indicates the part enlarged and shown in the following panel).

the range of few hundreds of nm, with 50–100 pA currents ($\sim 5 \times 10^{11}$ particles/s); for example, at CIBA (Centre for Ion Beam Applications of the National University of Singapore) a $290 \times 450\,\mathrm{nm}^2$ spot size with a 50 pA current of 2 MeV protons was obtained by using a triplet of compact quadrupoles [13]. These performances in the beam dimensions reduction are reached in a vacuum set-up. At the LABEC we have an external microbeam (fig. 2c) in order to exploit the advantages of out-of-vacuum set-up; in this configuration the lateral straggling of the beam due to the scattering with the atoms of the material of the window and of atmosphere gases sets a lower limit to the attainable spot size [14]. The lateral straggling in atmosphere can be reduced by positioning the sample as close as possible to the window. The minimum target-to-window distance depends on the detection angle of the detectors: the final part of the line does not have to intercept the solid angle under which the detectors see the impact point of the beam on the sample. Due to this constraint, in our set-up this distance is normally set at 2 mm [15]. Moreover, in order to limit the beam spread, we saturate the path in atmosphere with a light gas, such as helium, in which the extent of lateral straggling is smaller than in air. As far as the lateral straggling in the window is concerned, it is evident that the use of an ultra-thin window reduces this effect; we typically use, for our external microbeam, Si_3N_4 windows([1]) that have a 100 nm thickness. The combined use of a very thin window together with a very short path in helium atmosphere permits to reach very small probe dimensions, even working out of vacuum. At the LABEC microbeam [16] we can reach a spot size on sample well within 10 μm FWHM for standard 3 MeV protons.

2˙2. *Scanning system.* – To control the beam position on sample surface we have a system integrating a couple of coils, (fig. 2b) for beam displacements on target by magnetic deflection of the ions (magnetic scan), with a precision multi-axes stage (25 mm travel range) for high-resolution translation (reproducibility of position better than 1 μm) of the sample on the x-y plane (normal to beam) under fixed beam (mechanical scan) [16].

Magnetic scan allows us to raster the area of interest on sample more rapidly than the mechanical scan, but the maximum dimensions of this area are limited by the width of the beam exit window, usually $1 \times 1\,\mathrm{mm}^2$. To scan wider surface with limited time consuming we use the scanning system in "integrated" modality: a pattern of stage positions is communicated to the system and, for each stage position, a magnetic scan is performed.

2˙3. *Beam charge monitoring.* – The beam charge measure to determine the number of particles hitting the target is a key feature for quantitative analyses, to precisely control the degree of material modification and to study the effects of the radiation damage. The system we implemented uses a compact Si-PIN Photodiode ((P) in fig. 3) to detect the yield of Si X-rays produced by the beam in the exit window as an indirect measurement of the charge [17]. With a beam current of 1 nA over a 100 nm thick window membrane, we have a count rate of about 2 kHz due to Si X-rays; this allows us to measure the integrated charge in short times even with very weak currents (*e.g.* with a 10 pA current, less than 1 min is sufficient to have over one thousand counts on the Si X-ray normalisation peak). To check the reliability of the system and to calibrate it, we measured the ratio of the Si X-ray yield ($A_{\text{X-Si}}$) to the integrated charge Q_I for different beam current values, measured in a Faraday cup surrounding the window. As a result of an extensive series of

([1]) The Si_3N_4 windows are commercialized by Structure Probe Inc.; more information can be found on the web-site `www.2spi.com/spihome.html`.

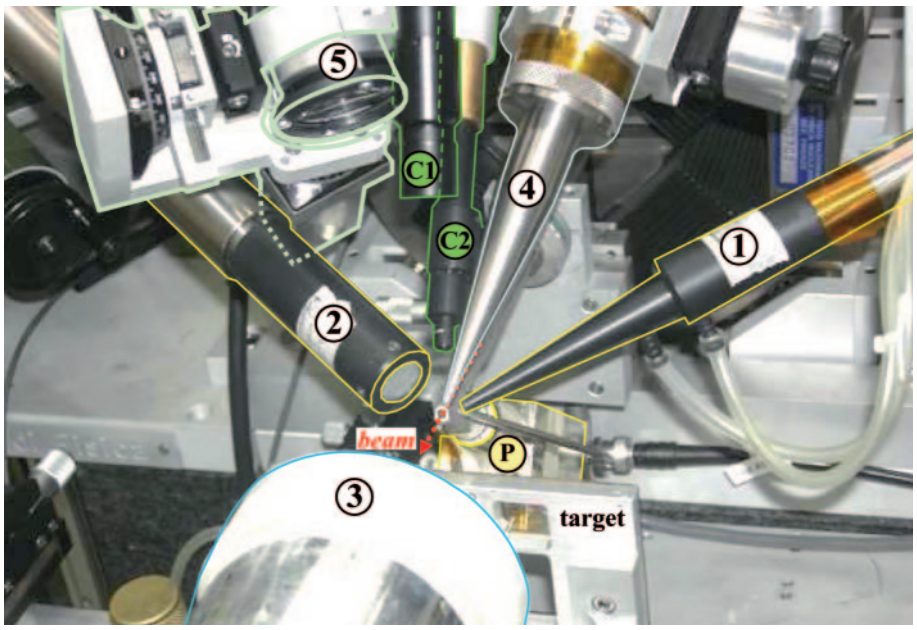

Fig. 3. – Beam end. (1) and (2): X-ray detectors optimized for low-medium– and medium-high-energy X-rays detection (PIXE); (3) γ-ray detector (PIGE); (4) vacuum-tight case containing the Si-photodiode for the detection of particles backscattered by the target (BS); (5) lens for light collection (IL); (P) Si-PIN detector for beam charge measure; (C1) and (C2) cameras for panoramic and microscopic sample visualization.

tests, we verified that, for a given window, the $A_{\text{X-Si}}/Q_I$ ratio keeps constant within 1%, varying the current of two orders of magnitude, from $\sim 10\,\text{nA}$ down to $\sim 100\,\text{pA}$ [16].

3. – IBA microanalyses at LABEC and examples of applications

3˙1. *External IBA set-up with mapping capability.* – The detection set-up of the LABEC microbeam allows us to analyse a sample in atmosphere by using simultaneously different IBA techniques: Particle-Induced X-ray Emission (PIXE), Particle-Induced γ-ray Emission (PIGE), Backscattering Spectroscopy (BS) and Ion-Beam–Induced Luminescence (IBIL or IL), based on the detection of characteristic X-rays, γ-rays, beam particles backscattered from the target and the light produced by the impinging particles in semiconductor/insulating materials, respectively. In our set-up [16, 18, 19] we use (see fig. 3):

– two X-ray detectors, (1) and (2) in fig. 3, optimized for low-medium– and medium-high–energy X-rays detection;

– a high-purity γ-ray germanium detector ((3) in fig. 3), placed just behind the sample to maximize the subtended solid angle;

– a Si-PIN windowless photodiode detector to detect recoiling particles, which is mounted in a vacuum-tight case ((4) in fig. 3) to minimize energy straggling along the particle path toward the detector;

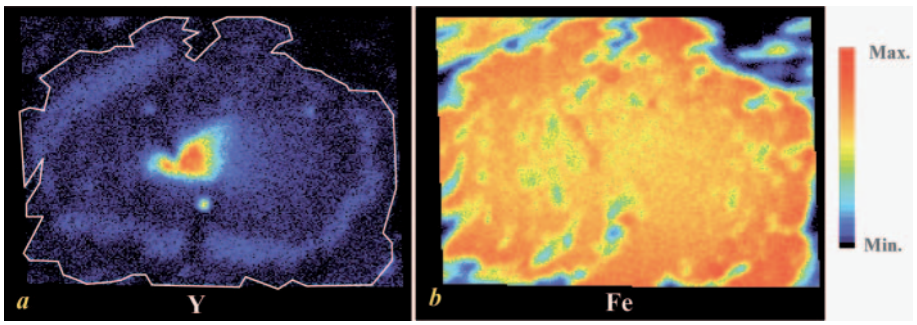

Fig. 4. – PIXE distrubution maps of yttrium (a) and iron (b) in one of the analysed garnet crystals (the white line in (a) represents the crystal perimeter).

– a CCD-based spectrometer (for spectra collection in real time) and a photomultiplier (for higher light collection efficiency) receiving the light from an optical collector ((5) in fig. 3) through an optical fiber.

The data acquisition software controls the scanning system thus making possible the collection of 2D maps of structural and compositional information on the area scanned by the beam, by means of the association of the measured energy of detected radiation or particle with the x-y position of the beam on sample surface at the moment of the detection.

Summarizing, our set-up allows a full characterization of samples in atmosphere through the collection of 2D maps of structural and compositional information of sample surface up to $25 \times 25\,\mathrm{mm}^2$ by exploiting simultaneously, PIXE, PIGE, BS and IL techniques.

Hereafter some examples of application in different fields are briefly described.

3˙2. *Examples of applications*

Earth science

A relevant research activity in Earth science aims at obtaining information about the structure and chemistry of the Earth's internal layers and about the evolution of the crust and mantle from the study of samples collected near the surface. The electron microprobe (EMP) has been the most used tool for this research, allowing quantitative microanalyses of major and minor elements. However, many elements of interest are present in trace (concentrations lower than 100 ppm) and remain below the detection limit of the electron microprobe. The nuclear microprobe is suited for studies of geological samples where microanalysis of trace elements is required [20].

One of the applications performed at LABEC concerning Earth science problems dealt with micro-PIXE analyses of garnet crystals, coming from the Calabrian-Peloritanian Arc (Southern Italy), to determine the distribution of yttrium, which is in concentrations down to tens of ppm [21]. The determination of the Y content in the garnets allows us to reconstruct the thermal history of the host rock, by applying the Y geothermometer, a phenomenological law describing an inverse relationship between rock formation temperature and maximum Y concentration. The micro-PIXE measurement of Y concentration revealed a marked zoning with higher concentrations in correspondence to the core of the garnet crystal (fig. 4a), thus resulting in a garnet growth occurred at different

temperatures, lower at the beginning than at the end. It is not possible to obtain analogous information from major elements because their zoning results characterized by a smoothed variation due to their high level of intra-crystalline diffusion (in fig. 4b is reported iron map as an example of the major element distribution); this made unfeasible the use of alternative techniques such as the EMP.

We performed analogous measurements on rutile crystals from the western Alps (Italy) to determine the zirconium content and apply the Zr-geothermometer [22].

We dated rocks coming from the Dora Maira Massif (Western Italian Alps) with the method of U-Th-Pb ratios applied to monazite crystals, by PIXE measurements of the U, Th and Pb concentrations [23]. The dating principle of U-Th-Pb in U and/or Th-containing minerals is that their progressive decay leads to an accumulation of Pb isotopes, so that the abundance ratios Pb/U and Pb/Th are a function of the time elapsed from the crystal formation, in the hypothesis, verified, that no exchanges of these elements with environment have taken place since formation, *i.e.* the system has been "closed".

We carried out the analysis of the elemental composition of the fluid included in tiny vacuoles (tens of micrometers) inside quartz crystals coming from the Apuan Alps metamorphic complex [24]. The results, although preliminary, were of interest for our geologist colleagues, as they gave useful information on the processes controlling the fluid compositions and on the source of some elements dissolved in the fluids circulating during the metamorphic processes of the Apuan Alps.

Our microbeam facility was also used for PIXE measurements of major, minor and trace element abundances in volcanic-rock sections from Nyiragongo Volcano (Democratic Republic of Congo), as explained in ref. [25].

Cultural heritage

Measurements of material composition in the field of cultural heritage are useful both for an advancement of the knowledge of materials and production technologies of art manufacts in ancient times, and for the investigation of materials prior to restorations of specific objects, to appropriately choose the restoring procedure, and avoid incompatibilities and irreversible effects. In this context, IBA techniques are known to play an outstanding role because they feature quantitative character, very high sensitivity and multi-element capability in a completely non-invasive and non-damaging way, without any sampling, owing to the possibility of performing analysis in an external set-up. The mapping capability with a good spatial resolution represents a crucial improvement in material composition measurements on works of art, since most of the objects of artistic or historical interest present inhomogeneous structures—on a scale of hundred micrometers or so—even within apparently uniform areas. In these cases, a "point" analysis can result in misleading information on the quantitative composition of the analysed sample. This risk can be avoided using a scanning approach, reconstructing compositional maps within the whole probed area, and extracting *a posteriori* information only from areas of interest [26].

In the past few years important works of art have been analysed at the microbeam facility of our laboratory, including paintings, metal-point drawings, "gold lace embroideries" from the Middle Ages and Renaissance and precious lapis lazuli artworks.

We performed PIXE investigations on the painting "Ritratto Trivulzio" by Antonello da Messina, one of the great Italian masters of the XV century. Elemental maps from selected areas helped to understand the way some colour shades had been obtained on the red mantle of the portrayed gentleman, using different pigments irregularly distributed on the surface. The obtained results provided to restorers and art historians useful

information on paint layer structure and composition that helped to identify materials and painting techniques used by Antonello [27].

We also performed measurements on metal-point drawings. In this particular form of art, flourished in Italy and northern Europe during the Renaissance, drawings are sketched, by means of a metal stylus, on paper covered by a pigment-based layer. Famous artists such as Leonardo, Raffaello, Botticelli, Dürer, widely used this technique. The knowledge of the materials used for both paper preparation and metal stylus is crucial to solve conservation problems of these precious and frail artworks. In these drawings, it is the non-uniformity of the track left by the stylus that makes the point compositional analysis by IBA problematic, especially when the same elements are present in both track and paper preparation. Indeed, the track is often composed of metal agglomerates with dimensions well below the millimetre scale. Therefore, a non-destructive imaging technique, with a spatial resolution of the order of 100 μm, is of great help for a correct characterisation of material composition. We performed PIXE measurements on sample drawings supplied by restorers of the Opificio delle Pietre Dure in Florence for a test analysis. Results reported in ref. [26] show how elemental maps are well suited for the unambiguous determination of the materials of the stylus.

The artworks known as "gold lace embroideries" are made with particular kinds of threads, in which a core composed of a silk fibre is spiral wrapped by a sort of miniature golden tape, the thickness of which may range from some micrometres to a few tens of micrometres. They were widely used in Europe from the Middle Ages to the eighteenth century to embellish embroideries in textile works of art or in fabrics to be used in important circumstances. There exist interesting archaeometrical problems related to these fabrics: learning about the production techniques and the materials of the golden or gilded tape, discriminating original embroideries from later mends and making decisions about restorations. The use of our external scanning microbeam allowed us to overcome difficulties in the analysis of this kind of samples related to the spatial non-homogeneity of the material and the non-planarity of the surface on scale lower than few hundreds of micrometres. In the frame of collaboration with the Opificio delle Pietre Dure in Florence, we analysed, by PIXE, a "gold lace embroidery" after a cartoon by Raffaellino del Garbo, a Florentine painter of the early Renaissance. We characterized structure and composition of the metal threads, which come out to be constituted by a very thin layer of gold (about 50 nm thick) on a Ag-Cu layer (about 8 μm thick) (for details see ref. [28]). Reference [29] reports on an analogous analysis performed on gold lace embroideries in a relic of St. Francis.

Recently we have started a provenance study of the lapis lazuli stone, which was largely used in the past for the production of valuable objects of art, such as jewels, amulets, seals, and inlays, and, from the sixth century B.C. until the last centuries, for the preparation of a precious blue pigment known as "lapis lazuli blue". The stone of lapis lazuli is a fine grain (down to tens of micrometers) aggregate of different minerals: lazurite, the main component responsible of the blue coloration, and a calcium/magnesium silicate network. In order to find provenance markers in elemental composition, by PIXE/PIGE, or in light response, by IL, the use of a scanning microbeam is important to discriminate the contribution of the different mineral phases of the rock. We performed the first measurements on raw lapis lazuli samples of different known origins and on precious lapis lazuli artworks of the Collezione Medicea of Museum of Natural History, University of Florence (fig. 5) [30, 31].

The work is still in progress but the results are promising and the experimental differences among different known-origin samples are significant (for details see ref. [32]).

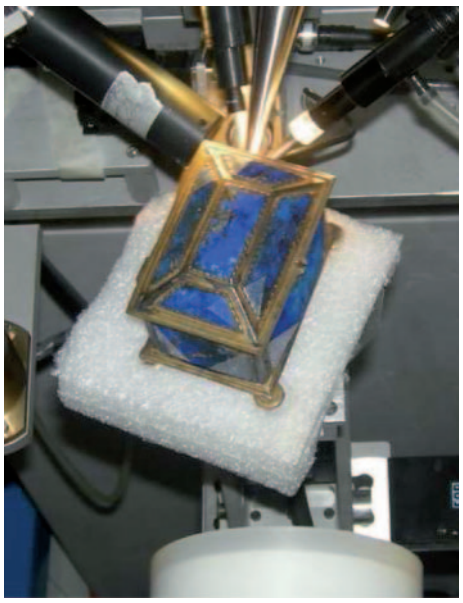

Fig. 5. – "Bauletto", cat. N. [13684] from the "Collezione Medicea di Pietre Ornamentali", Mineralogy and Lithology section of the Museum of Natural History, University of Florence, during the positioning for the analyses at the microbeam of LABEC.

Technological applications

An IBA technique commonly used to characterise the electronic properties of semiconductor devices is the IBIC (Ion-Beam–Induced Charge collection). IBIC is used with rarefied beam (thousands of particles per second) and is based on the detection and analysis of the charge signals induced in the material by the impinging particles. Mapping capability is required to investigate possible spatial variations in the electronic response of the device.

Recently we performed an IBIC analysis to investigate the electronic properties of a thin-film solar cell [33]; this kind of solar cells has the great advantage of being much easier and cheaper to produce in comparison to those of crystalline silicon. The active element of the analysed device consists in a heterojunction of a $\sim 100\,\text{nm}$ thick CdS layer (n-type semiconductor) and $\sim 10\,\mu\text{m}$ thick CdTe layer (p-type semiconductor). The IBIC measurements were carried out using He ions raster scanned onto the surface to obtain the map of the charge collection efficiency (CCE) of the device. The collected CCE maps showed inhomogeneous response of the cell to be attributed to the polycrystalline nature of the CdTe. In addition, the evolution of the IBIC signal *vs.* the ion fluence was studied in order to evaluate the radiation hardness of the CdS/CdTe solar cells, in view of their use in solar modules for space applications.

At the microbeam of Florence we carried out a micro-PIXE analysis on pitch adapters of the electronics of the silicon tracker for the Compact Muon Solenoid (CMS experiment of LHC) [34]. A pitch adapter consists of a fan of very thin chromium strips coated with a few micrometers aluminium deposition, on a glass support. Our analysis was focused on the Al deposition since the micro-bonds had shown mechanical and electrical problems. The measurements pointed out a significant copper contamination of the metal deposition indicating the role of Cu impurities in the encountered problems during micro-bonding.

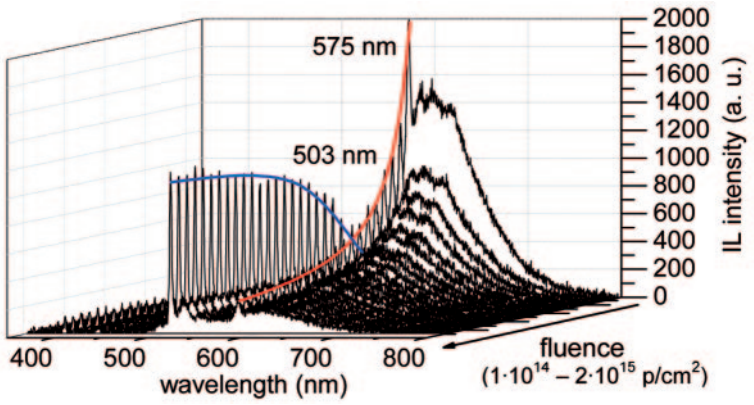

Fig. 6. – Three-dimensional plot of IL spectra at increasing fluences of 2 MeV protons in the $1 \cdot 10^{14}$–$2 \cdot 10^{15}$ p/cm^2 range; the rapid decrease of the emission of the luminescence center at $\lambda = 575$ nm is clearly visible, as well as the increase in the emission of the center at $\lambda = 503$ nm.

4. – Irradiation on diamond: first applications in the material modification field

In the search of a reliable platform for a scalable fabrication technology of quantum devices, diamond is attracting growing interest. The micro-fabrication methods are based on the creation of structural defects in the crystal structure, often induced by the use of ion beams, in order to produce monolithic photonic devices. The control on the variation of the refractive index as a function of structural damage/disorder induced by the ions is a key parameter for this kind of advanced photonics applications. Moreover, with the aim of the fabricating photonic devices in bulk diamond, the low-contrast refractive index modulation induced by ion implantation, instead of merely being a side effect, could play an active role in the design of the device.

Monoenergetic implantations with MeV light ions, such as hydrogen or helium, induce the formation of modified regions lying under the diamond surface, at a depth and with a thickness depending on energy and kind of ion. The depth can vary from few micrometers to tens of micrometers, depending on the ion stopping range, and the thickness ranges from hundreds of nanometers to few micrometers, depending on the Bragg peak width of the damage profile. The MeV ion microbeam can be an extremely versatile tool to locally modify the optical properties of materials with micrometric spatial resolution both in the lateral and depth directions.

We started a systematic study of the effects of MeV-ion-beam–induced structural damage on the refractive index in single-crystal CVD diamond. First results, obtained using 2 and 3 MeV protons in the fluence range 10^{15}–10^{17} cm^{-2}, show an approximately linear increasing behaviour of the refractive index with the fluence (for details see ref. [35]).

We also studied the effects of the ion damage in diamond on its luminescence properties. Diamond features a large variety of luminescence centers which, when irradiated, emit light with characteristic wavelength. The luminescence centers define diamond optical properties and can be either created or modified by irradiation damage. We started this study by performing IL measurements on single-crystal CVD diamond samples irradiated by 2 MeV protons in order to investigate the radiation hardness of several of such centers as a function of the implanted fluence. Some results are shown in fig. 6: a rapid

decrease of the emission of the luminescence center at $\lambda = 575\,\text{nm}$ is clearly visible, as well as an increase in the emission of the center at $\lambda = 503\,\text{nm}$ (for details see ref. [36]).

5. – Conclusions

The external scanning ion microbeam in Florence is a well-established instrument to be applied in a large variety of fields, such as earth sciences, material science and cultural heritage. Concerning the analysis of materials, it is possible to characterize samples in atmosphere by extracting maps of elemental and structural information obtained by simultaneous PIXE, BS, PIGE and IL measurements; the beam scanning system allows us to collect 2D maps over an area up to $25 \times 25\,\text{mm}^2$ and with the strong focusing system it is possible to reach a spatial resolution better than $10\,\mu\text{m}$, while maintaining all the attractive aspects of an external set-up.

So far, we have used the facility mainly for analyses of materials, but recently we also open up to ion modification of materials; the first results obtained in the modification of diamond for future developments in advanced optical-device production appear to be promising.

* * *

The author is deeply indebted with his co-workers Dr. L. Giuntini and Dr. S. Calusi in the research activity at the LABEC microbeam facility and with the entire LABEC group for the fruitful collaboration in many steps of the work here summarized. Many thanks also to all the researchers who were involved in the applications performed at the microbeam of Florence. The financial support was mainly given by the INFN. The author wishes to warmly thank M. Falorsi, A. Catelani and M. Manetti for skilful suggestions and careful mechanical developments, R. Ciaranfi and M. Montecchi for the assistance with the electronics and G. Tobia for valuable help in the detector set-up.

REFERENCES

[1] Nastasi M., Tesmer J. R. (Editors), *Handbook of Ion Beam Materials Analysis* (Materials Research Society, Pittsburg) 1995.
[2] Johansson S. A. E., Campbell J. L. and Malmqvist K. G. (Editors), *Particle Induced X-ray Emission (PIXE)* (John Wiley & Sons Inc., Chichester) 1995.
[3] Chu W.-K., *Backscattering Spectroscopy* (Academic Press) 1978 ISBN-10: 0121738507 ISBN-13: 978-0121738501.
[4] Mandò P. A., *Nucl. Instrum. Methods B*, **85** (1994) 815.
[5] Watt F. and Grime G. W., *High-energy Ion Microbeams* (Adam Hilger, Bristol) 1987.
[6] van Kan J. A., Bettiol A. A. and Watt F., *Appl. Phys. Lett.*, **83** (2003) 1629.
[7] Ortega R., Devès G. and Moretto Ph., *Nucl. Instrum. Methods B*, **181** (2001) 475.
[8] `http://www.microbeams.co.uk/`.
[9] Ryan C. G. and Jamieson D. N., *Nucl. Instrum. Methods B*, **158** (1999) 997.
[10] Dollinger G. *et al.*, *Nucl. Instrum. Methods B*, **210** (2003) 6.
[11] Pehrson G. R. *et al.*, *Nucl. Instrum. Methods A*, **609** (2009) 294.
[12] Merchant M. J. *et al.*, *Nucl. Instrum. Methods B*, **260** (2007) 8.
[13] Watt F. *et al.*, *Nucl. Instrum. Methods B*, **210** (2003) 14.
[14] Moliere G., *Z. Naturforsch.*, **3a** (1948) 78.
[15] Massi M., Giuntini L., Chiari M., Gelli N. and Mandò P. A., *Nucl. Instrum. Methods B*, **190** (2002) 276.
[16] Giuntini L., Massi M. and Calusi S., *Nucl. Instrum. Methods A*, **576** (2007) 266.

[17] Calligaro T., Dran J.-C., Ioannidou E., Moignard B., Pichon L. and Salomon J., *Nucl. Instrum. Methods B*, **161-163** (2000) 328.
[18] Calusi S., Colombo E., Giuntini L., Lo Giudice A., Manfredotti C., Massi M., Pratesi G. and Vittone E., *Nucl. Instrum. Methods B*, **266** (2008) 2306.
[19] Colombo E., Calusi S., Cossio R., Giuntini L., Lo Giudice A., Mandò P. A., Manfredotti C., Massi M., Mirto F. A. and Vittone E., *Nucl. Instrum. Methods B*, **266** (2008) 1527.
[20] Ryan C. G., *Nucl. Instrum. Methods B*, **104** (1995) 377.
[21] Borghi A., Compagnoni R., Cossio R., Giuntini L., Massi M., Olmi F., Santo Alba P. and Vaggelli G., *Microchim. Acta*, **155** (2006) 105.
[22] Vaggelli G., Borghi A., Calusi S., Cossio R., Giuntini L. and Massi M., *X-Ray Spectrom.*, **37** (2008) 146.
[23] Vaggelli G., Borghi A., Cossio R., Fedi M. E., Giuntini L., Lombardo B., Marino A., Massi M., Olmi F. and Petrelli M., *Microchim. Acta*, **155** (2006) 305.
[24] Massi M., Calusi S., Giuntini L., Ruggieri G. and Dini A., *Nucl. Instrum. Methods B*, **266** (2008) 2371.
[25] Santo A. P., Fedi M. E., Giuntini L., Mandò P. A., Massi M. and Taccetti F., *Microchim. Acta*, **155** (2006) 263.
[26] Grassi N., Giuntini L., Mandò P. A. and Massi M., *Nucl. Instrum. Methods B*, **256** (2007) 712.
[27] Grassi N., *Nucl. Instrum. Methods B*, **267** (2009) 825.
[28] Migliori A., Massi M. and Giuntini L., *Surf. Eng.*, **24** (2008) 98.
[29] Migliori A., Grassi N. and Mandò P. A., *Nucl. Instrum. Methods B*, **266** (2008) 2339.
[30] Calusi S., Colombo E., Giuntini L., Lo Giudice A., Manfredotti C., Massi M., Pratesi G. and Vittone E., *Nucl. Instrum. Methods B*, **266** (2008) 2306.
[31] Colombo E., Calusi S., Cossio R., Giuntini L., Lo Giudice A., Mandò P. A., Manfredotti C., Massi M., Mirto F. A. and Vittone E., *Nucl. Instrum. Methods B*, **266** (2008) 1527.
[32] Lo Giudice A., Re A., Calusi S., Giuntini L., Massi M., Olivero P., Pratesi G., Albonico M. and Conz E., *Anal. Bioanal. Chem.*, **395** (2009) 2211.
[33] Colombo E., Bosio A., Calusi S., Giuntini L., Lo Giudice A., Manfredotti C., Massi M., Olivero P., Romeo A., Romeo N. and Vittone E., *Nucl. Instrum. Methods B*, **267** (2009) 2181.
[34] Massi M., Giuntini L., Fedi M. E., Arilli C., Grassi N., Mandò P. A., Migliori A. and Focardi E., *Nucl. Instrum. Methods B*, **722** (2004) 219.
[35] Olivero P., Calusi S., Giuntini L., Lagomarsino S., Lo Giudice A., Massi M., Sciortino S., Vannoni M. and Vittone E., *Diam. Relat. Mater.*, **19** (2010) 428.
[36] Manfredotti C., Calusi S., Lo Giudice A., Giuntini L., Massi M., Olivero P. and Re A., *Diam. Relat. Mater.*, **19** (2010) 854.